Calculation of free-free Gaunt factors in hot dense plasmas

I. J. Feng,* M. Lamoureux,† and R. H. Pratt
Department of Physics and Astronomy, University of Pittsburgh, Pittsburgh, Pennsylvania 15260

H. K. Tseng
Department of Physics, National Central University, Chung-Li, Taiwan 320, Republic of China
(Received 20 September 1982)

We have obtained predictions for free-free Gaunt factors, using a full relativistic numerical partial-wave and multipole calculation of the bremsstrahlung process as a single electron transition in a potential. We study hot dense cesium plasmas, at various densities and temperatures, using the finite-temperature and -density Thomas-Fermi potential. We consider incident electron energies in the range 1–50 keV. Our results show that use of isolated neutral or ion Gaunt factors has only limited applicability in this environment, while use of the Elwert-Born approximation can lead to a factor-of-3 discrepancy for low incident electron energies.

I. INTRODUCTION

The bremsstrahlung (free-free) process is important in transport problems involving hot dense plasmas.[1] Bremsstrahlung emission by superthermal electrons from laser irradiated targets is also a useful diagnostic in laser-plasma interaction experiments.[2] Measurement of bremsstrahlung emission by less energetic electrons gives information on the temperature gradients in the critical region of laser fusion plasmas.

Earlier calculations of free-free Gaunt factors (ratio of the free-free cross sections to those predicted by Kramers's classical evaluation) have been performed within the Born approximation or nonrelativistic dipole approximation, and for the pure Coulomb,[3] Debye-Hückel,[4,5] ion-sphere,[6] Thomas-Fermi,[7] and average-atom potentials.[8] Recently[9] we have reported a sample full relativistic calculation for the process, considered as a single electron transition in the Thomas-Fermi potential, with partial wave and multipole expansions, for incident electron energy $\epsilon=1$ keV, for a Cs plasma at $kT=1$ keV, at the density $\rho=\rho_0$ ($\rho_0=1.9$ g/cm$^3=0.86\times10^{22}$ atoms/cm^3 is the normal density). In this work, we extend our study to include the ranges $\epsilon=1-50$ keV for a Cs plasma with $kT=0.1-1$ keV, density $\rho/\rho_o=1-100$. This allows us to understand the behavior of free-free Gaunt factors for some of the presently important ranges in incident electron energy ϵ, plasma temperatures kT, and densities ρ.

We find that, as temperatures decrease or densities increase, the value of Gaunt factors decrease, since electron density in the interior region of the atom increases and the potential becomes more screened. The characterization of the spectrum by that of an isolated atom or ion can be misleading near the soft-photon end, and it is also inappropriate when densities become so high that the potential can be even more screened than in the neutral-atom case. Elwert-Born (EB) approximation is poor at low incident electron energies (1 keV) where a factor-of-3 error can occur, while at higher energies (e.g., 50 keV) it gives satisfactory results.

In Sec. II we describe our method of calculation. In Sec. III we present our average atom finite temperature and density central potentials and compare them with isolated free neutral-atom and ion potentials. In Sec. IV we report the free-free Gaunt factors we obtain in various Cs plasmas and compare them with isolated atom and ion predictions. We also discuss the validity of Born-Elwert approximation predictions. In Sec. V we give Gaunt factors averaged over a thermal distribution of incident electron kinetic energies, for a few sample cases.

II. METHODS OF CALCULATION

In our full relativistic numerical calculation[10] of the bremsstrahlung process, we assume that the process may be described as a single electron transition in a self-consistent potential, with partial-wave expansions for the electron wave functions in the potential and a multipole expansion for the radiated photon. For isolated atom or ion cases, the relativistic Hartree-Fock potentials with local Kohn-Sham

exchange (HFS potentials) are used. However for Cs, the difference between the zero-temperature isolated atom Thomas-Fermi potential and the Hartree-Fock neutral-atom potential is rather small in the dominant region of the bremsstrahlung process at these energies, hence the differences between the two energy spectra are also small. For the cases of hot dense plasmas, we describe an average atom in the plasma with the Thomas-Fermi model.[11] The Thomas-Fermi model provides a quantitative prediction for heavy atoms in hot dense plasmas and the numerical procedures are relatively simple. In either situation, the reduced photon-energy spectrum $\sigma=\beta_i^2\omega Z^{-2}d\sigma/d\omega$ is obtained by evaluating the relativistic matrix element

$$M_{fi}\propto\int\psi^*\vec{\alpha}\cdot\vec{\epsilon}^*e^{-i\vec{k}\cdot\vec{r}}\psi_i d^3r\ ,$$

where $\beta_i=v_i/c$, with v_1 and v_2 the incident and final velocity and $\hbar\omega$ the photon energy radiated. Results for the cross section σ are often expressed in terms of the free-free Gaunt factor $g(\epsilon,\hbar\omega)$, defined as $\sigma/\sigma_{\rm Cl}$, where $\sigma_{\rm Cl}=5.61$ mb is Kramers's semiclassical result.

The nonrelativistic Elwert-Born (EB) approximation is known to be valid for neutral atoms when the incident electron energy $\sim\beta_i^2$ is high enough compared with atomic-field-potential energies in this region of radiation but is not yet in the relativistic regime.[12] (Relativistic EB approximation is valid in the relativistic domain, but only for light-Z elements.) The Gaunt factor in nonrelativistic Born approximation is

$$g_B(\epsilon,\hbar\omega)=\frac{\sqrt{3}}{\pi Z^2}\int_{q_{\rm min}}^{q_{\rm max}}[2\pi^2V(q)]^2q^3dq\ , \tag{2.1}$$

where $V(q)=(2\pi)^{-3}\int V(r)e^{i\vec{q}\cdot\vec{r}}d^3r$ is the Fourier transform of the potential $V(r)$. Note that $V(q)\propto q^{-2}F(q)$ where the form factor $F(q)$ is the Fourier transform of the corresponding charge distribution. The quantities $q_{\rm min}$ and $q_{\rm max}$ are the minimum and maximum momentum transfers to the atom. When defined nonrelativistically by assuming energy conservation in radiation of a photon of energy $\hbar\omega$

$$\left.\begin{matrix}q_{\rm max}\\ q_{\rm min}\end{matrix}\right\}=(2\epsilon)^{1/2}\pm[2(\epsilon-\hbar\omega)]^{1/2}\ . \tag{2.2}$$

The Elwert-Born Gaunt factor is $g_{\rm EB}(\epsilon,\hbar\omega)=g_B(\epsilon,\hbar\omega)f_E$, where the Elwert factor f_E is

$$f_E=\frac{\beta_1}{\beta_2}\frac{1-\exp(-2\pi Z\alpha/\beta_1)}{1-\exp(-2\pi Z\alpha/\beta_2)}\ . \tag{2.3}$$

The simplified form $f_B\sim v_2/v_1$ is valid[12] if $2\pi Z\alpha/\beta_i>3$ or if $v_1\sim v_2$.

For the Coulomb case, at low energies EB predicts a tip value $\sigma=6.2$ mb, not too different from Kramers's predictions; the logarithmic divergence at the soft-photon end is also common to all calculations. However, throughout most of the spectrum EB gives a poor result in the classical regime. For the neutral-atom case, in the classical regime where EB is no longer valid, the EB form-factor approximation also fails. Comparisons of EB results with numerical neutral-atom and Coulomb data were given by Lee *et al.*[13] Their data show, for example, that for $Z=79$ and $\epsilon=5$ keV, EB form factor overestimates the neutral-atom value by a factor of 2 at the soft-photon end and 40% at the tip. Our results for the dense plasma case (Sec. IV) indicate a similar trend of error in EB form-factor predictions.

For many practical purposes, such as determinations of emission and absorption coefficients,[14] one is interested not in cross sections but in rate coefficients, and particularly in the rate coefficients $\langle\sigma v\rangle$, which are averaged over the energy distribution of the free electron in the plasma at the temperature T. In the case of a Maxwellian distribution these will be expressed in terms of the dimensionless averaged Gaunt factor

$$\bar{G}(\hbar\omega)=\frac{1}{kT}\int_{\hbar\omega}^{\infty}g(\epsilon,\hbar\omega)e^{-\epsilon/kT}d\epsilon\ . \tag{2.4}$$

Since $\bar{G}=e^{-\hbar\omega/kT}$ when $g=1$ (Kramers value) this factor is often removed in defining an average Gaunt factor $\bar{g}$ related to $\bar{G}$ by

$$\bar{g}(\hbar\omega)=e^{\hbar\omega/kT}\bar{G}(\hbar\omega)\ , \tag{2.5}$$

so that $\bar{g}=1$ when the Kramers formula is used for the basic spectrum. Note that for degenerate plasmas, we would have to replace the exponential in the integral above by $\{\exp[(\epsilon-\mu)/kT]+1\}^{-1}p(\epsilon,\hbar\omega)$, corresponding to the Fermi-Dirac distribution.

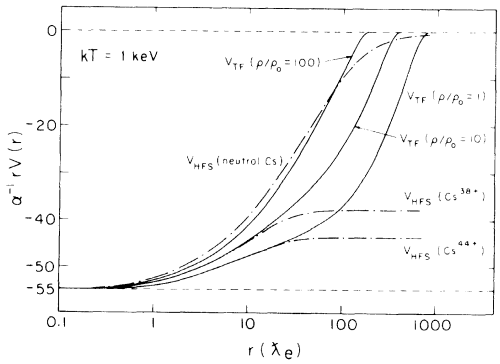

FIG. 1. Comparison of TF potentials with isolated atom or ion potentials for Cs ($Z=55$), for $kT=1$ keV, $\rho/\rho_0=1$, 10, 100. We plot rV, which goes to $Z=55$ for $r=0$ and to 0 (neutral case) or the ionic charge for large distances.

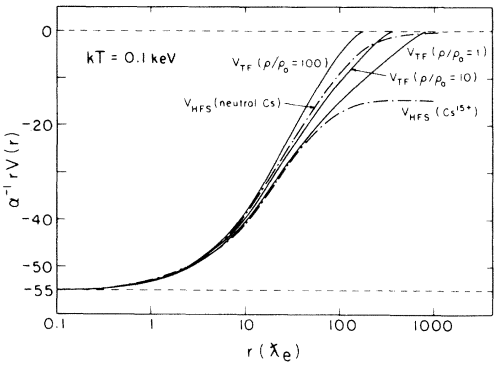

FIG. 2. Same as Fig. 1, except for $kT=0.1$ keV.

Here the factor p measures the availability of final states:

$$p(\epsilon,h\omega)=\frac{\exp[(\epsilon-\hbar\omega-\mu)/kT]}{\exp[(\epsilon-\hbar\omega-\mu)/kT]+1} . \quad (2.6)$$

The chemical potential μ of the free electron is obtained automatically in the Thomas-Fermi model when the equations for the potential are solved.

III. RESULTS FOR TEMPERATURE AND DENSITY DEPENDENCE OF ATOMIC POTENTIALS

In Figs. 1 and 2, we show comparisons of Thomas-Fermi potentials at various densities and temperatures with isolated Cs neutral-atom and ion potentials. The Thomas-Fermi (TF) potential vanishes at the atom boundary, at the radius r_a for the confined atom determined from the ion number density n_i as $r_a=(3n_i/4\pi)^{-1/3}$. The degree of ionization Z^* at finite temperature and density has been calculated in the TF model, using a standard identification[5] of Z^* with the ratio of free-electron density at the atom boundary to the average electron density,

$$Z^*=\frac{n_e(r_a)}{Zn_i} .$$

Our Z^* values agree with Rozsnyai's finite temperature full Hartree-Fock-Slater calculation[8] within 10% for the temperature and density range considered here.

For small distances from the atomic nucleus, say of the order of ten electron Compton wavelength, the TF potentials for various temperatures and densities are nearly the same as the potentials for isolated Cs ions with corresponding degrees of ionization Z^*. For example (see Figs. 1 and 2), for a Cs plasma at a temperature $kT=1$ keV, density $\rho/\rho_o=1$, for r up to $15\lambda\!\!\!^{-}_e$, the TF potential is almost the same as a Cs, $_{11}$Na-like ion. For a Cs plasma with $kT=0.1$ keV, $\rho/\rho_0=1$, for r up to $20\lambda\!\!\!^{-}_e$, the TF potential is very close to that of a Cs, $_{40}$Zr-like ion.

However, we note that for very high densities, at least for $\rho/\rho_0\gtrsim 100$, even at quite small distances the TF potential is not like the potential of the corresponding isolated ion with Z^* calculated as above, but is closer to the shape of a potential for an isolated ion with a smaller degree of ionization. And, more strikingly, when the density is high enough and/or the temperature is low enough, the potential is less attractive than in the neutral case. An illustration of this situation is shown in Fig. 2 in the case of a cesium plasma with $kT=0.1$ keV and $\rho/\rho_0=100$. In other words, the atom has been pressure rather than temperature ionized, and the continuum states are more confined, more completely screening the nucleus, than in the isolated neutral-atom case. We will see a coresponding behavior for Gaunt factors in the next section.

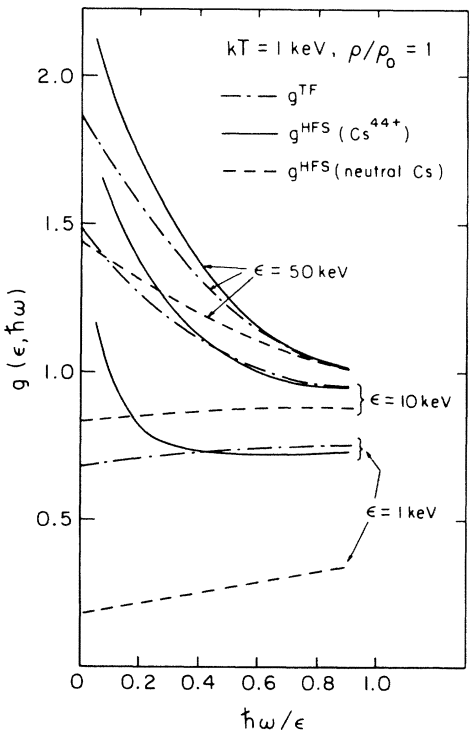

FIG. 3. Free-free Gaunt factors obtained by full relativistic calculation in TF potentials (g^{TF}), as a function of $\hbar\omega/\epsilon$ (ratio of photon energy radiated to incident electron kinetic energy) for Cs plasmas at $kT=1$ keV, $\rho/\rho_0=1$, for incident electron energies $\epsilon=1$, 10, and 50 keV, compared with isolated neutral-atom or ion (Cs^{44+} is Na-like) results.

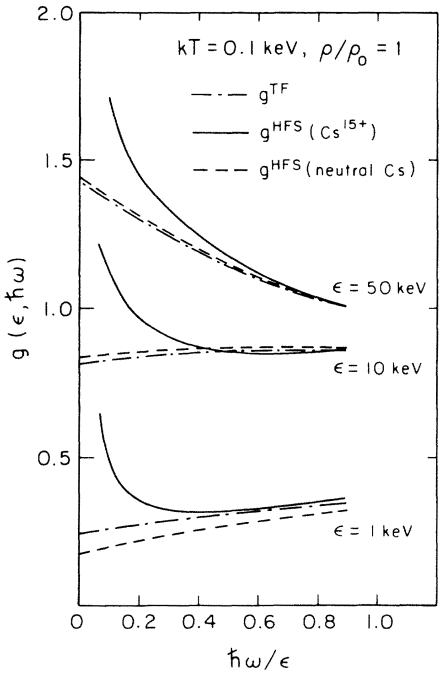

FIG. 4. Same as Fig. 3, except for $kT=0.1$ keV, and compared with Cs^{15+} (Zr-like) ion results.

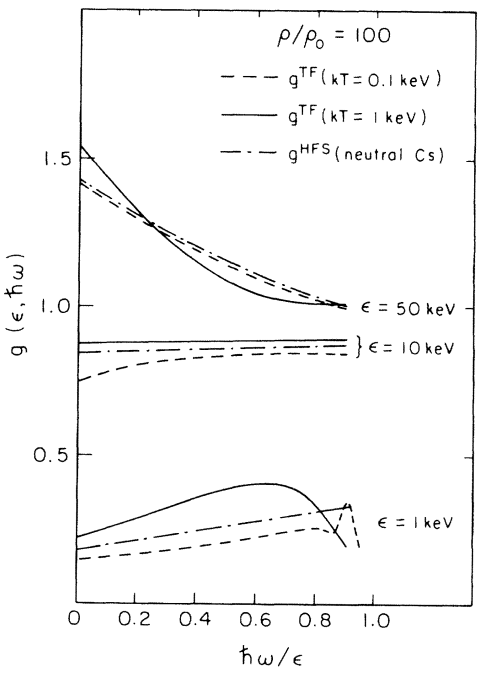

FIG. 5. Same as Fig. 3, except for $kT=0.1$ keV, and $\rho/\rho_0=100$, compared with neutral-atom results.

IV. RESULTS FOR TEMPERATURE AND DENSITY DEPENDENCE OF FREE-FREE SPECTRA

In Figs. 3 and 4 we show the Gaunt factors of electron bremsstrahlung for Cs plasmas at density ρ/ρ_0, temperatures 0.1 and 1 keV, compared with isolated neutral-atom and ion results. We see that for $\rho/\rho_0=1$, for a large portion of the spectrum ($\hbar\omega/\epsilon \gtrsim 0.5$), $g^{\mathrm{TF}}(Z,kT,\rho)$ is very close to $g(Z^*)$, the Gaunt factor of the isolated ion whose degree of ionization Z^* is determined from the Thomas-Fermi model. The explanation of this result is that the bremsstrahlung process is determined at relatively small distances from the nucleus for these energies, except near the soft-photon end and at low energies. At these distances we have seen the similarity in the shapes of TF and isolated ion potentials. Figure 3 shows that for $\rho/\rho_0=1$, $kT=1$ keV, the curves for g^{TF} lie higher than those for the isolated neutral atom, more significantly at low energies. However, Fig. 4 shows that for $\rho/\rho_0=1$, $T=0.1$ keV, the neutral-atom results, although not quite as good as the isolated ion (Cs^{15+}) results for $\hbar\omega/\epsilon \gtrsim 0.5$, give a satisfactory prediction for g^{TF}, throughout the studied range of kinetic energy ϵ, for the whole spectrum (i.e., for the soft- as well as the hard-photon portions). These features can be understood in terms of the behaviors of the corresponding potentials.

Figure 5 shows the Gaunt factors for $\rho/\rho_0=100$, $kT=0.1$ and 1 keV, compared with neutral-atoms results. We see that at this high density the spectrum exhibits different features. g^{TF} for $kT=0.1$ keV generally lies below the neutral Cs curve, owing to the fact that the corresponding potential is more screened than in the neutral case. Another striking feature is the shape resonance[15] observed for $\epsilon=1$ keV case, near the hard-photon end at $\hbar\omega/kT \simeq 0.9$. This corresponds to a continuum electron energy of around 100 eV in the $\kappa=-3$ channel. For isolated neutral-atom cases, pronounced shape resonances[16] usually do not occur except for final electron energies in the eV range. However, for very compressed atoms, the potentials cut off more steeply than in the neutral-atom cases, so that the shape resonance phenomenum can occur at higher final electron energies. Such a shape resonance is exposed when the incident electron energy is low, because then higher partial waves in the final state contribute to the spectrum. We also notice that the $\epsilon=1$ keV curve for $kT=1$ keV, at this density, exhibits a great curvature, which has not been seen in neutral-atom or ion cases. This results from a reduced normalization (small-distance magnitude) of low-energy continuum waves which do not penetrate through the more compact screening into the interior attractive nuclear charge. This drop is also seen in the $\epsilon=1$

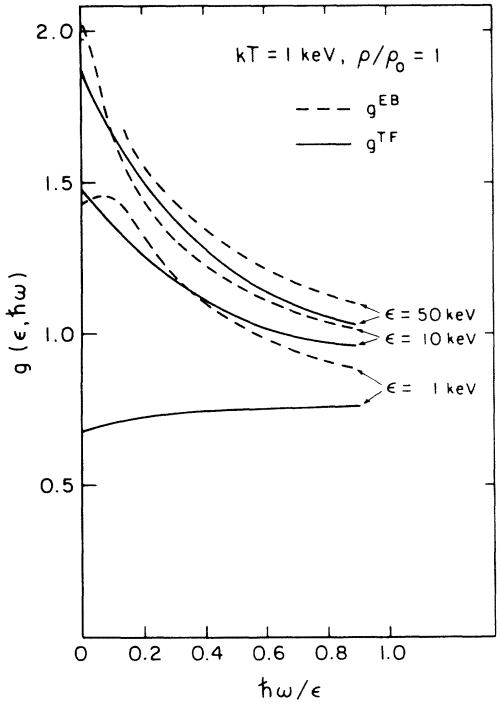

FIG. 6. g^{TF} compared with results obtained from EB approximation (g_{EB}), for $kT=1$ keV, $\rho/\rho_0=1$.

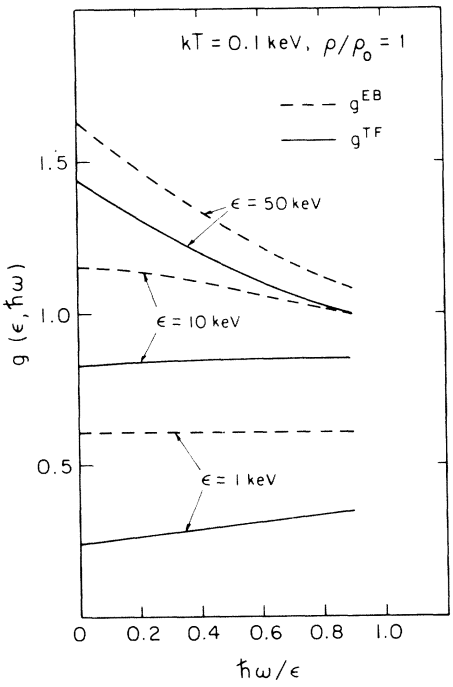

FIG. 8. Same as Fig. 6, except for $kT=0.1$ keV, and $\rho/\rho_0=1$.

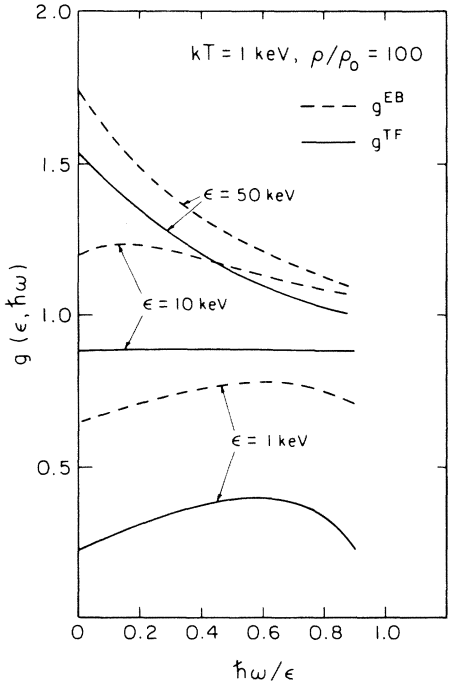

FIG. 7. Same as Fig. 6, except for $kT=1$ keV, and $\rho/\rho_0=100$.

keV spectrum at $kT=0.1$ keV for this density (Fig. 5), beginning at about $\hbar\omega/\epsilon\simeq 0.8$, but then the shape resonance is superimposed. (For the less compact isolated neutral atom case, only in the last tens of eV will the spectrum start dropping as low-energy screened continuum normalizations begin to differ substantially from Coulomb.)

In Figs. 6–9 we again show these partial wave results for the bremsstrahlung Gaunt factors, for $kT=0.1$ and 1 keV and densities $\rho/\rho_0=1$ and 100, for incident electron energies $\epsilon=1$, 10, and 50 keV, now in comparison with the results from Elwert-Born approximation. Generally speaking, independent of temperature and density through these ranges, for $Z=55$ EB approximation is valid for $\epsilon=50$ keV, accurate within 30% for $\epsilon=10$ keV, and becomes inaccurate for $\epsilon=1$ keV where a factor-of-3 error can occur. It is clear that, as in the neutral case, use of EB approximation becomes inappropriate at low energies.

V. THERMAL ELECTRON DISTRIBUTION AVERAGED GAUNT FACTORS

We have estimated the frequency dependence of thermal electron distribution averaged Gaunt factors for several sample cases for $\hbar\omega=1$ and 5 keV, at

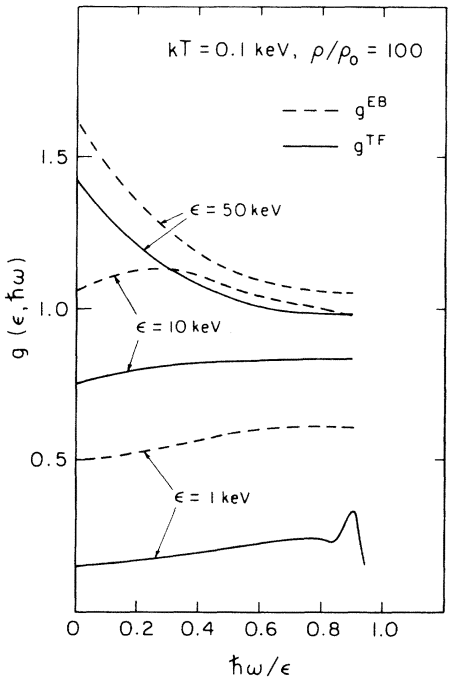

FIG. 9. Same as Fig. 6, except for $kT=0.1$ keV, and $\rho/\rho_0=100$.

density $\rho/\rho_0=1$, for $kT=0.1$ and 1 keV. Under these conditions, we can assume the electrons in the plasma have a Maxwellian distribution. Owing to the factor $\exp(-\epsilon/kT)$ in Eq. (2.4) when $\hbar\omega \gtrsim kT$ the contribution to $\bar{g}(\hbar\omega)$ comes mostly from $g(\epsilon,\hbar\omega)$ with $\epsilon\sim\hbar\omega$. The tip region of the spectrum thus plays a dominant role in the average, and generally $g(\hbar\omega,\hbar\omega)$ is an estimate (and an underestimate) of $\bar{g}(\hbar\omega)$, as shown in Table I. Hence the bremsstrahlung spectrum can be characterized by the corresponding isolated ion spectra, when they are similar away from the soft-photon end as in Figs. 3 and 4. In these circumstances we use the simple parametrization of bremsstrahlung spectra for isolated atoms and ions, developed recently by Feng and Pratt,[12] to generate values of Gaunt factors for the corresponding ion, at many different values of incident electron energies for a given photon energy $\hbar\omega$, and then perform the thermal distribution average. We have checked values for Gaunt factors obtained with this parametrization g^P against our available numerical data $g^{\rm TF}$, and we find that in the worst case the agreement is within 20% (e.g., for $\rho/\rho_0=1$, $kT=0.1$ keV, $\hbar\omega=1$ keV, and $\epsilon=1$ keV we have $g^{\rm TF}=0.35$, and $g^P=0.28$). This parametrization method can be applied even near the soft-photon end, where the (flat) high-$T\rho$ behavior differs from the ln divergence of the isolated ion, since the parametrization underestimates the isolated ion Gaunt factors and still agrees quite well with $g^{\rm TF}$. We believe the overall error in this estimate of averaged Gaunt factors should be less than 15%, and this is supported by a consideration of direct estimates of $\bar{g}$ by interpolation from the very limited $g^{\rm TF}$ data.

Karzas and Latter[3] (KL) have calculated temperature averaged free-free Gaunt factors $\bar{g}^{\rm KL}$ within the nonrelativistic dipole (Coulomb) approximation, covering a wide range of temperatures and photon energies $\hbar\omega$. In Table I we compare our estimated $\bar{g}$ with those presented by Karzas and Latter, under the assumption that the nuclear charge Z is used in their expression. At these temperatures and photon energies, $\bar{g}^{\rm KL}$ is of the order unity. However our results show that $\bar{g}$ is significantly smaller than $\bar{g}^{\rm KL}$, especially for cases where the potential is more screened and/or for smaller photon energies where the contribution comes mainly from low-energy incident electrons.

For $\hbar\omega \gtrsim 10$ keV and at not too high a density, $\bar{g}$ should have a value approaching unity, as the screening effect becomes less important, while nonrelativistic dipole approximation remains valid for the spectrum and over most of the spectrum the Kramers formula is a good approximation to the Sommerfeld formula. Green[7] has calculated $g(\epsilon,\hbar\omega)$ for a gold plasma, using nonrelativistic dipole approximation in the TF potential, and noted

TABLE I. Comparison of temperature averaged free-free Gaunt factors $\bar{g}$ calculated from the parametrized g^P of Ref. 12 with results obtained by Karzas and Latter, $\bar{g}^{\rm KL}$. To show that for these cases the tip region of the spectrum plays a dominant role in the averaged free-free Gaunt factors $\bar{g}$, we also present in the table the values of $g^P(\hbar\omega,\hbar\omega)$.

$Z^*=44$, $kT=1$ keV, $\rho/\rho_0=1$				$Z^*=15$, $kT=0.1$ keV, $\rho/\rho_0=1$			
$\hbar\omega$ (keV)	$\bar{g}$	$\bar{g}^{\rm KL}$	$g^P(\hbar\omega,\hbar\omega)$	$\hbar\omega$ (keV)	$\bar{g}$	$\bar{g}^{\rm KL}$	$g^P(\hbar\omega,\hbar\omega)$
1	0.80	1.15	0.69	1	0.30	1.07	0.28
5	0.98	1.12	0.93	5	0.77	1.07	0.76

that for $\epsilon \sim kT$, $g(\epsilon,\hbar\omega) \simeq (Z^*/Z)^2$ over most of the spectrum. If this argument is valid, then we would expect $\bar{g} \simeq (Z^*/Z)^2$ for $\hbar\omega \sim kT$. This is in agreement with our result for $\bar{g}$ at $\rho/\rho_0 = 1$, $\hbar\omega = \mathrm{kT} = 1$ keV [$\bar{g} = 0.80$ and $\bar{g}^{\mathrm{KL}}(Z^*/Z)^2 = 0.74$].

For $\hbar\omega/kT \ll 1$, $\bar{g}$ in the Coulomb case diverges logarithmically (as a function of $\hbar\omega/kT$ for a given kT), since the contribution is mainly from electron energies $\epsilon/kT \lesssim 1$, at the soft-photon end of the resulting spectra, which in the Coulomb case diverge logarithmically.[17] For the screened case, we would expect that $\bar{g}$ decreases as $\hbar\omega$ decreases. A nonrelativistic dipole calculation in the screened TF (rather than Coulomb) potential is required to show this behavior of $\bar{g}$.

ACKNOWLEDGMENTS

The authors wish to thank B. Sundaram for his assistance in numerical computations, and Dr. I. Goldberg for his help in clarifying the calculation of normalization and phase shifts of low-energy electron wave functions. This work is supported in part by the National Science Foundation (U.S.) under Grant No. PHY-81-20675 and in part by the National Science Council of the Republic of China. One of us (M.L.) acknowledges her stay at the University of Pittsburgh, which was due to a National Science Foundation—Centre National de la Recherche Scientifique exchange program.

---

*Present address: Bell Telephone Laboratories, Murray Hill, New Jersey 07971.

†Permanent address: Laboratoire de la Spectroscopie Atomique et Ionique, Bâtiment 350, Université Paris-sud, F-91405 Orsay, France.

[1]For a recent review, see R. M. More, in Applied Collision Physics, edited by C. J. Barnett (Academic, New York, in press), Vol. II.

[2]K. A. Brueckner, in *Laser Induced Fusion and X-Ray Laser Studies,* edited by S. J. Jacobs (Addison-Wesley, Reading, Mass., 1976); K. A. Brueckner and Y. T. Lee, Nucl. Fusion 19, 1431 (1979); P. Jaegle, A. Carillon, G. Jamelot, and Cl. Wehenkel, Conf. on Atomic Processes in High Temperature Plasmas, Baton Rouge, LA (1981) p. 36.

[3]W. J. Karzas and R. Latter, Astrophysics J. Suppl. 6, 167 (1961).

[4]J. M. Green, R. and D. Associates (Santa Monica, California) Report No. RDA-TR-4900-007 (unpublished).

[5]I. P. Grant, Mon. Not. R. Astron. Soc. 118, 241 (1958).

[6]H. Zirin, Astrophys. J. 119, 371 (1954).

[7]J. M. Green, R. and D. Associates (Santa Monica, California) Report No. RDA-TR-237-AEC (unpublished).

[8]B. F. Rozsnyai, J. Quant. Spectrosc. Radiat. Transfer 22, 337 (1979).

[9]M. Lamoureux, I. J. Feng, R. H. Pratt, and H. K. Tseng, J. Quant. Spectrosc. Radiat. Transfer 27, 227 (1982).

[10]H. K. Tseng and R. H. Pratt, Phys. Rev. A 3, 100 (1971).

[11]R. F. Feynman, N. Metropolis, and E. Teller, Phys. Rev. 75, 1561 (1949); R. Latter, *ibid.* 99, 510 (1955). We have verified that a numerical calculation of the spectrum in a potential corresponding to Rozsnyai's fitted two Yukawa potentials (Ref. 8) yields results similar to those with our Thomas-Fermi potential.

[12]I. J. Feng and R. H. Pratt, University of Pittsburgh, Report No. PITT-266 (unpublished).

[13]C. M. Lee, Lynn Kissel, R. H. Pratt, and H. K. Tseng, Phys. Rev. A 13, 1714 (1976).

[14]I. I. Sobelman, L. A. Vainshtein, and E. A. Yukov, *Excitation of Atoms and Broadening of Spectral Lines* (Springer, Berlin, 1981); G. Bekefi, *Radiation Processes in Plasmas* (Wiley, New York, 1966).

[15]J. M. Green has also observed shape resonance in the free-free Gaunt factor: J. M. Green, R. and D. Associates (Santa Monica, California) Report No. RDA-TR-4900-002 (unpublished). These were calculated within the nonrelativistic dipole approximation for Debye-Hückel potentials.

[16]C. M. Lee and R. H. Pratt, Phys. Rev. A 12, 707 (1975).

[17]W. H. Tucker, *Radiation Processes in Astrophysics* (MIT, Cambridge, Mass., 1975), Chap. 5.